PHYSICAL REVIEW E, VOLUME 65, 035101(R)

Nonuniversality of invasion percolation in two-dimensional systems

Mark A. Knackstedt,[1,2] Muhammad Sahimi,[3,4] and Adrian P. Sheppard[1,2]
[1]*Department of Applied Mathematics, Research School of Physical Sciences and Engineering, Australian National University, Canberra ACT 0200, Australia*
[2]*Australian Petroleum Cooperative Research Centre, University of New South Wales, Sydney, NSW 2052, Australia*
[3]*Department of Chemical Engineering, University of Southern California, Los Angeles, California 90089-1211*
[4]*Institute for Advanced Studies in Basic Sciences, Gava Zang, Zanjan 45195-159, Iran*
(Received 21 June 2001; published 7 February 2002)

Employing highly efficient algorithms for simulating invasion percolation (IP) with trapping, we obtain precise estimates for the fractal dimensions of the sample-spanning cluster, the backbone, and the minimal path in a variety of two-dimensional lattices. The results indicate that these quantities are nonuniversal and vary with the coordination number Z of the lattices. In particular, while the fractal dimension D_f of the sample-spanning cluster in lattices with low Z has the generally accepted value of about 1.82, it crosses over to the value of random percolation, $D_f \simeq 1.896$, if Z is large enough. Since optimal paths in strongly disordered media and minimum spanning trees on random graphs are related to IP, the implication is that these problems do not also possess universal scaling properties.

DOI: 10.1103/PhysRevE.65.035101 PACS number(s): 64.60.Ak, 47.55.Mh

Multiphase flow phenomena in porous media are relevant to many problems of great scientific and industrial importance, including extraction of oil, gas, and geothermal energy from underground reservoirs, food and soil sciences, powder technology, and materials science [1]. Invasion percolation (IP), a model introduced [2] for describing the evolution of the interface between an invading and a defending fluid in a porous medium, has provided deep insight into such phenomena. In addition, IP is relevant to a host of other problems, including characterization of optimal paths and domain walls in strongly disordered media [3,4], minimum spanning trees [5], and even simulation of the Ising model at the critical temperature [6]. Moreover, IP is one of the simplest parameter-free models which exhibits self-organized criticality [7], another subject of current interest.

Two main variants of IP have been studied so far. In nontrapping IP (NTIP) the defending fluid is compressible and the invading fluid can potentially enter any region on the interface which is occupied by the defending fluid. In the second and more common case, the trapping IP (TIP) which is the subject of this paper, the defending fluid is incompressible and is trapped if a portion of it is surrounded by the invading fluid. In addition to the compressibility, one must also take into account the ability of the fluids to wet the internal surface of the medium [1]. In imbibition a wetting fluid is drawn spontaneously into a porous medium, while during drainage a nonwetting fluid is pushed into the pore space. We model the porous medium as a network of pores or sites connected by throats or bonds which have smaller radii than the pores. In IP, the potential displacement events are ranked according to the capillary pressure threshold that must be exceeded before that event takes place. During imbibition, the invading fluid is drawn first into the smallest constrictions, for which the capillary pressure is large and negative, and it goes last into the widest pores. Displacement events are therefore ranked in terms of the largest opening that the invading fluid must travel through, since it is from these larger capillaries or bonds that it is most difficult to displace the defender. Imbibition is therefore a *site* IP, whereas drainage in which the invader has most difficulty with the smallest constrictions is a *bond* IP.

Important differences arise [4,8–11] in the structure of the invading fluid paths, depending on whether one considers NTIP or TIP. The scaling properties of NTIP are believed to be consistent with those of random percolation (RP). On the other hand, up until now it has been assumed that the scaling properties of TIP in two dimensions (2D) are universal and independent of the lattice type, and distinct from those of RP. The purpose of this paper is to report the results of extensive simulation of TIP in 2D in a variety of lattices which indicate that, contrary to the common belief, the scaling properties of this model are all nonuniversal and lattice dependent. Since the scaling properties of IP are related to those of optimal paths in random media and the geometry of minimum spanning trees on random graphs, the universality of the scaling properties of these phenomena, which has been claimed in the past [3–5], is also questioned.

Since the differences between values of various scaling exponents of TIP and RP appear to be small, it is critical to be able to simulate very large lattices in order to establish the universality classes of TIP models. We have recently developed [11] a highly efficient algorithm for simulating TIP in which the simulation time grows as $O[N \ln(N)]$, where N is the number of sites in the lattice, which enables us to simulate very large lattices for measuring the scaling properties of TIP models with very high accuracy. Briefly, in this algorithm one looks for the trapped regions by searching the neighbors of each newly invaded site. If trapping is possible, then several simultaneous breadth first ''forest-fire'' searches are used to update the cluster labeling as necessary [8], which restricts the changes to the most local region possible. Since during an invasion each site can be invaded or trapped at most once, this part of the algorithm scales as $O(N)$. The search is done for cluster volumes rather than perimeters and

TABLE I. Values of the three fractal dimensions on various 2D lattices. All the results were obtained with $L\times L$ lattices, unless specified otherwise. Numbers in parentheses indicate the estimated error in the last digit.

	D_f	D_{bb}	$D_{\min}$
Site NTIP	1.8959(1)	1.6432(8)	1.1307(4)
Site TIP			
Hexagonal	1.831(6)	1.21(2)	1.218(6)
Square	1.825(4)	1.22(2)	1.214(1)
Triangular	1.890(2)	1.616(2)	1.132(7)
Triangular ($L\times 2L$)	1.892(2)	1.617(2)	1.137(3)
Star	1.896(1)	1.642(2)	1.136(3)
Star ($L\times 2L$)	1.895(2)	1.642(4)	1.133(3)
Bond TIP			
Hexagonal	1.831(6)		1.218(6)
Square	1.822(8)		1.214(2)
Triangular	1.823(2)		1.215(1)
Star	1.895(7)		1.221(3)

incorporates local checking to minimize cluster searching, and is thus equally effective in 3D.

We also store the sites (bonds) on the fluid-fluid interface in a list, sorted according to the capillary pressure threshold needed to invade them. This list is implemented via a balanced binary search tree, so that insertion and deletion operations on the list can be performed in $\log(n)$ time, where n is the list size. Sites (bonds) that are designated trapped using the above described procedures are removed from the invasion list. Each site is added and removed from the interface list at most once, limiting the cost of this part of the algorithm to $O[N\log(n)]$. Thus the execution time for N sites (bonds) is dominated (for large N) by list manipulation and scales *at most* as $O[N\ln(N)]$.

We have also used a different optimized algorithm [11] to identify the minimal path length, the sites comprising both the elastic backbone [12], i.e., the set of the sites that lie on the union of all the shortest paths between two widely separated points, and the usual transport backbone, so that the backbone search and computations do not affect the overall execution time of the algorithm. Although numerous algorithms have been proposed in the past [12,13], as we have discussed elsewhere [11], our algorithm appears to be more efficient than the previous methods. Briefly, the algorithm consists of four steps. (i) Using a breadth-first search algorithm, we label each site in the cluster with its ''cluster distance'' from the inlet face, and then use this information to burn backwards from the outlet face and identify the elastic backbone. We also construct the ''branch points list''—a list of all the cluster sites that are adjacent to the elastic backbone but are not part of it. The branch points list should be ordered with the sites closest to the inlet face listed first. (ii) The search stops if the branch points list is empty. Otherwise, a depth-first search from the last site in the branch points list is performed, flagging all the sites that are visited. During the search, unexplored branch points are added to the branch points list, while another list tracks the sites that have been flagged as visited. We then carry out an optimization during the depth-first search: If there are multiple branches from a single site, the site labeled as the closest to the inlet face is always the first to be explored. (iii) The depth-first search terminates when one of two conditions are satisfied: (1) The search contacts the backbone again at a different site from where it started, in which case the sites in the visited-sites list are flagged as backbone sites, or (2) it retreats back to its starting site, at which point there will be no sites left in the visited-sites list. (iv) The algorithm continues at step (ii).

We carried out extensive simulations using the hexagonal, square, triangular, and star lattices, thus spanning a range of coordination numbers Z ranging from $Z=3$ for the hexagonal lattice to $Z=8$ for the star lattice, which is constructed by adding diagonal bonds to the square lattice. We simulated both site and bond TIP using $L\times L$ lattices with reflecting boundary conditions on the edges. In the case of the triangular and star lattices, we also used $L\times 2L$ lattices and measured the cluster properties within the central $L\times L$ region (see below). Lattice sizes ranging from $L=16$ to $L=8192$ were used. The number of realizations varied between 5×10^6 for $L=16$ to 3000 for $L=8192$, representing the most extensive TIP simulations that we are aware of.

Consider, for example, the fractal dimension D_f of the sample-spanning cluster. If we define a local fractal dimensions $D_f(M)\equiv d\ln M/d\ln L$ (where M is the mass of the cluster), then according to finite-size scaling (FSS) $D_f(M)$ converges to its asymptotic (large M) value as $|D_f-D_f(M)|\sim M^{-\alpha}$, where α is a correction-to-scaling exponent. Combining the definition of $D_f(M)$ with the FSS equation yields a differential equation which has an analytical solution [11]:

$$c_1+D_fM^{\alpha}=c_2L^{\alpha D_f}, \tag{1}$$

where c_1 and c_2 are two constants. We thus fit the data to Eq. (1) to estimate both D_f and α simultaneously. Equations similar to Eq. (1) are also used for estimating D_{bb} and $D_{\min}$

(and the corresponding αs), the fractal dimensions of the backbone and the minimal paths, respectively.

Table I presents the results for both site and bond TIP in the four lattices that we used. The estimated values of D_f in the hexagonal and square lattices in both site and bond TIP are completely consistent with each other and with the generally accepted value [11], $D_f \simeq 1.825 \pm 0.004$, obtained in the square lattice. For bond TIP the estimated D_f in the triangular lattice is also consistent with this value. However, for site TIP, the value of D_f in the triangular lattice jumps to about 1.890 ± 0.002, just outside $D_f = 91/48 \simeq 1.8958$ for RP. To obtain a more accurate estimate, we used $L \times 2L$ triangular lattices and collected statistics in the middle $L \times L$ part in order to eliminate boundary effects. We obtained $D_f \simeq 1.892 \pm 0.002$, which is again slightly outside the value for RP. Although this estimate is extremely accurate, we cannot completely rule out the possibility that with even larger lattices one would obtain a value of D_f which is completely consistent with that of RP. However, in the case of the star lattice, both site and bond TIP have a value of D_f that is completely consistent with RP.

The same trends are seen in the value of the backbone fractal dimension D_{bb}, namely, in the low-coordinated lattices D_{bb} takes on the value that we recently reported [11] for the square lattice, but as the coordination number of the lattice increases, so also does D_{bb}. The estimate for the star lattice is completely consistent with that of RP (Ref. [11] and Grassberger [13]), $D_{bb} \simeq 1.6432 \pm 0.0008$. However, our results for the triangular lattice consistently exhibit small but systematic and significant deviations from that of RP; see Table I. To show the quality of the data, we present them in Fig. 1, where we used $D_{bb} \simeq 1.617$, and the confidence ellipses [14] for the estimated exponents. Clearly, $M/L^{1.617}$ is converging to a constant value, while the confidence ellipses provide error estimates that are so small that rule out any significantly larger D_{bb}. The behavior of D_{bb}, which is consistent with that of D_f, might be indicative of one of the two scenarios. (1) There is in fact a *distinct* intermediate case between the low-and high-coordinated lattices represented by the triangular lattice. The distinct value of D_{bb} in the triangular lattice, as well as its estimated $D_{\min}$ discussed below, strongly support this scenario. (2) Alternatively, there may be only two distinct sets of fractal dimensions, one each for the low- and high-coordinated lattices, which are separated by a critical coordination number $6 \leqslant Z_c < 8$. If so, the convergence of the results for the triangular lattice to those of RP should be very slow; one must use much larger lattices in order to obtain the true asymptotic values. Although our results do not provide any significant support for this scenario, we cannot completely rule out this possibility.

Finally, the results for $D_{\min}$ for site TIP are completely consistent with the other two sets of results, namely, in low-coordinated lattices, the value of $D_{\min}$ are consistent with the previous estimate [11] reported for the square lattice, at the highest coordination number, it crosses over to that of RP (Grassberger [13]), $D_{\min} \simeq 1.1307 \pm 0.0004$, with the value for the triangular lattice being in between the two cases. However, with bond TIP, all the estimates of $D_{\min}$ are consistent with the previous value for the square lattice [11].

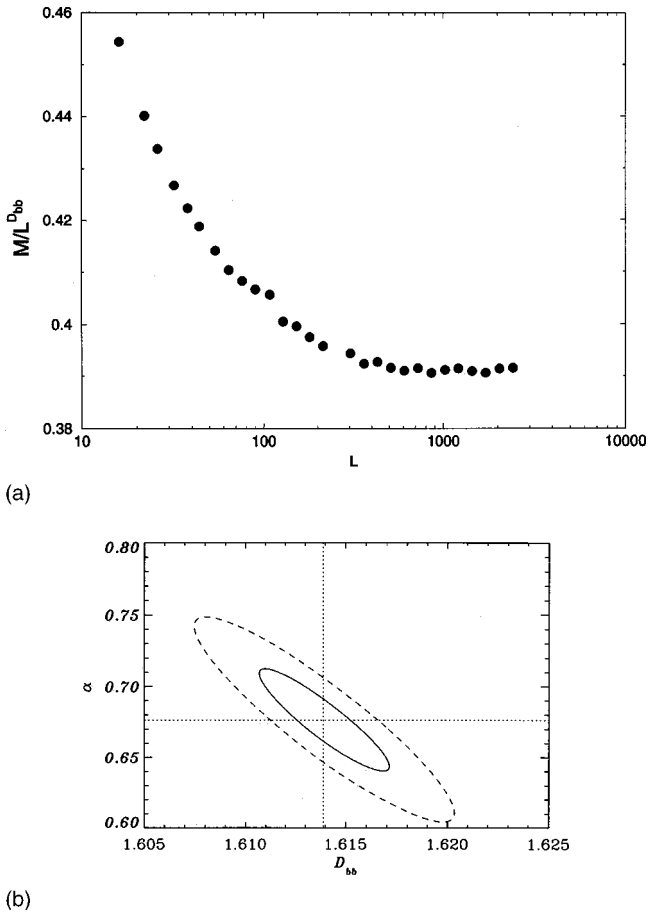

FIG. 1. (a) The behavior of the mass M of the backbone in the triangular lattice in site TIP versus its linear size L, where $D_{bb} \simeq 1.617$. (b) Confidence ellipses for the finite-size scaling exponent α and the fractal dimension D_{bb}. The solid (dashed) curve shows 68% (90%) confidence level.

Note that bond TIP has been claimed [3,4] to be in the universality of optimal paths in the limit of strong disorder [3], and as such it is expected to be different from site TIP. All the results together leave very little, if any, doubt that the scaling properties of TIP in 2D are lattice dependent, and hence nonuniversal. They also indicate that, contrary to common belief, site and bond TIP have quite different scaling properties.

Trapping IP is a dynamical process. It is already known [15] that diffusion-limited aggregation, another dynamical process, is also characterized by a lattice dependent fractal dimension. One may then ask whether such nonuniversality is a generic feature of some dynamical processes, and if so, what distinguishes those with universal properties from the ones with nonuniversal properties. In addition, since the scaling properties of IP are related to those of optimal paths in strongly disordered media [3,4] and minimum spanning trees on random graphs [5], contrary to the common belief, these problems must also have nonuniversal properties. It is possible that all of these phenomena have universal scaling

properties in the continuum limit which, however, have not been computed.

M.A.K. is grateful to the Australian Research Council for financial support. Work at USC was supported in part by the Petroleum Research Fund, administered by the American Chemical Society. We thank the ANU Supercomputing Facility and the High Performance Computing Facility at the University of Queensland for generous allocations of computer time.

[1] M. Sahimi, Rev. Mod. Phys. **65**, 1393 (1993); *Flow and Transport in Porous Media and Fractured Rock* (VCH, Weinheim, Germany, 1995).

[2] R. Chandler, J. Koplik, K. Lerman, and J. F. Willemsen, J. Fluid Mech. **119**, 249 (1982); D. Wilkinson and J. Willemsen, J. Phys. A **16**, 3365 (1983).

[3] M. Cieplak, A. Maritan, and J. R. Banavar, Phys. Rev. Lett. **72**, 2320 (1994); **76**, 3754 (1996).

[4] M. Porto, S. Havlin, S. Schwarzer, and A. Bunde, Phys. Rev. Lett. **79**, 4060 (1997); M. Porto, A. Bunde, S. Havlin, and H. E. Roman, Phys. Rev. E **56**, 1667 (1997).

[5] R. Dobrin and P. M. Duxbury, Phys. Rev. Lett. **86**, 5076 (2001).

[6] J. Machta, Y. S. Choi, A. Lucke, and T. Schweizer, Phys. Rev. Lett. **75**, 2792 (1995); G. Franzese, V. Cataudella, and A. Coniglio, Phys. Rev. E **57**, 88 (1998).

[7] C. P. Stark, Nature (London) **352**, 423 (1991); R. Cafiero, A. Gabrielli, M. Marsili, and L. Pietronero, Phys. Rev. E **54**, 1406 (1996).

[8] F. Babalievski, Int. J. Mod. Phys. C **9**, 43 (1998).

[9] A.-L. Barabási, Phys. Rev. Lett. **76**, 3750 (1996); S. Schwarzer, S. Havlin, and A. Bunde, Phys. Rev. E **59**, 3262 (1999), and references therein.

[10] M. Sahimi, M. Hashemi, and J. Ghassemzadeh, Physica A **260**, 231 (1998); E. Aker, K. J. Maaløy, and A. Hansen, Phys. Rev. Lett. **84**, 4589 (2000).

[11] A. P. Sheppard, M. A. Knackstedt, W. V. Pinczewski, and M. Sahimi, J. Phys. A **32**, L521 (1999); M. A. Knackstedt, M. Sahimi, and A. P. Sheppard, Phys. Rev. E **61**, 4920 (2000).

[12] H. J. Herrmann, D. C. Hong, and H. E. Stanley, J. Phys. A **17**, L261 (1984).

[13] C. Liem and N. Jan, J. Phys. A **21**, L243 (1988); M. D. Rintoul and H. Nakanishi, *ibid.* **27**, 5445 (1994); P. Grassberger, Physica A **262**, 251 (1999); J. Phys. A **25**, 5477, 5867 (1992); C. Moukarzel, Int. J. Mod. Phys. C **9**, 887 (1998).

[14] W. H. Press, S. A. Teukolsky, W. T. Vetterling, and B. P. Flannery, *Numerical Recipes*, 2nd ed. (Cambridge University Press, Cambridge, England 1992), Chap. 15.

[15] L. A. Turkevich and H. Scher, Phys. Rev. Lett. **55**, 1026 (1985); Phys. Rev. A **33**, 786 (1986).